Synthesis of PVDF nanocomposite surface-modified membrane containing ZnO:Ca for dye removal from colored wastewaters in a fixed-bed photocatalytic-membrane reactor

Abbas Rajabi Abhari[a], Ali Akbar Safekordi[a], Mohammad Ebrahim Olya[b,*], Niyaz Mohammad Mahmoodi[b]

[a]_Department of applied Chemistry, Science and Research Branch, Islamic Azad University, Tehran, Iran,_
_emails: Abbas_Rajabi66@yahoo.com (A.R. Abhari), safekordi@sharif.edu (A.A. Safekordi)_
[b]_Department of Environmental Research, Institute for Color Science and Technology, Tehran, Iran, P.O. Box: 16765-654,_
Tel. +98 21 22944184; Fax: +98 21 22947537;
emails: olya-me@icrc.ac.ir (M.E. Olya), mahmoodi@icrc.ac.ir (N.M. Mahmoodi)

a b s t r a c t

In the present study, the process of synthesis of polymeric membranes based on polyvinylidene fluoride (PVDF) was investigated using different techniques of phase inversion and also the process of surface modification was carried out via chemical method with diethanolamine (DEA). Also, removal of Reactive Red 120 (RR120), Reactive Blue 19 (RB19), and Basic Violet 16 (BV16) from the synthetic effluent was evaluated in the dead-end membrane system. Results revealed that 20% w/w of polymer is suitable for production of a uniform film which is resistant against fluid pressure (2–4 bar). DEA optimal (%w/w) was determined about 20% to remove the fluorine atoms from the hydrocarbon chain in order to increase the hydrophilic properties of membrane. Furthermore, the nano-photocatalyst zinc oxide: calcium (ZnO:Ca) was synthesized by combustion method. The optimum value of ZnO:Ca nanoparticles to make a nanocomposite membrane (PVDF/ZnO:Ca) was 10% w/w. Findings showed that decolorization of RR120, RB19 and BV16 using membrane system was increased from 3.84%, 2.61% and 37.52% to 18.45%, 27.36% and 66.45%, respectively, within 2 h because of chemical modification and ZnO:Ca photocatalyst nanoparticles. In addition, the removal efficiencies of dyes in a fixed-bed photocatalytic-membrane reactor (FPMR) during 1 h were 65.10%, 75.95% and 65.04%, respectively. Finally, results indicated that FPMR has a high removal efficiency, compared with the other studied membrane systems.

Keywords: Fixed-bed PMR; Membrane; Surface chemical modification; Polyvinylidene fluoride

1. Introduction

Organic dyes applied in dyeing process of textile industries have detrimental effects on human health being, due to the presence of aromatic groups, heavy metals, chlorides and the other harmful substances. They could be released into the environment as industrial wastewaters which have undesirable and irreparable effects on aquatic life [1–3]. In addition, these compounds are carcinogenic, allergenic with mutagenic nature. The presence of these compounds in the human body, can cause serious problems in internal organs such as skin irritation, kidney failure, damage to the genital system, liver, brain and central nervous system and consequently endanger human health [4].

Organic dyes are designed and manufactured with high light stability, due to their application in the dyeing process. Among several classes of dyes, reactive dyes have about 50% of the global market and the most commonly used group as chromophore is the azo group followed by anthraquinone [5]. Some dyes, such as Reactive Red 120 (RR120) containing azo groups as chromophore and Reactive Blue 19 (RB19) that has an anthraquinone group in its chemical structure as chromophore, are among the most commonly applied dyes in the textile industries. Furthermore, Basic violet 16 (BV16) which is in the Methine class is used for dyeing paper and as a component inks for printing and ink-jet printers. According to the presence of sustained and resistant groups such as aromatic groups, these dyes have been shown highly resistant against degradation by microorganisms and in other words these compounds are no biodegradable [6]. It is also not possible to remove these dyes from effluents by conventional treatment techniques [7,8]. Nowadays, hybrid systems have attracted the attention of researchers more than ever because of the significant purification efficiency. A combination of membrane technology and a heterogeneous photocatalytic process in a hybrid system is called photocatalytic-membrane reactors (PMRs) [9,10]. In PMRs, the high oxidizing process of photocatalyst and powerful membrane separation could be achieved at the same time. These hybrid reactors have two general configurations including suspension (slurry) and fixed-bed [11]. In the slurry PMRs, the available nano-photocatalyst in the photo reactor after the process, the suspended nano-photocatalyst is separated from the treated water using membrane. This hybrid system is known as slurry photocatalytic-membrane reactors (SPMRs) [12]. Also, when nano-photocatalyst is stabilized in the membrane, the hybrid system is known as a fixed-bed photocatalytic-membrane reactor (FPMRs). Grzechulska-Damszel et al. [13] observed that the time of decolorization in SPMR was much shorter than FPMR. SPMRs to exhibited higher degradation performance, in comparison with FPMRs, because the available active sites at the nano-photocatalyst in SPMRs are more than FPMR. But, the main restriction of SPMRs is separation of nano-photocatalyst from the treated water at the end of process. In order to solve this problem, the application of FPMRs is a promising process for preserving nano-photocatalyst and preventing the extra stage of separation after the process. In FPMRs, the membrane is directly exposed to ultraviolet (UV) radiation, so the membrane constructor should be selected from non-degradable materials against ultraviolet (UV) radiation and oxidizing active species produced in the nano-photocatalytic process. In a research conducted by Chin et al. [14], the stability of 10 types of polymer membranes in the photocatalytic process was evaluated. Among them, polyvinylidene fluoride (PVDF) and polytetrafluoroethylene showed the highest stability, and poly propylene (PP) and cellulose acetate showed the lower stability. PVDF is a polymer that is classified into thermoplastics. This polymer has high mechanical strength and resistance to most chemical compounds such as organic and inorganic acids, aromatic and aliphatic hydrocarbons, alcohols, oxidants and many chemical solvents. It is also highly stable against UV radiation [15–17]. Accordingly, PVDF was selected as a membrane constructor in this study. But one of the most important problems in the commercialization of PVDF membranes is the obstruction
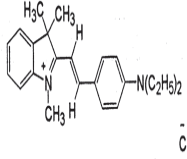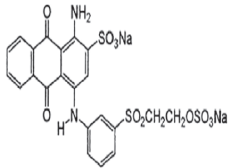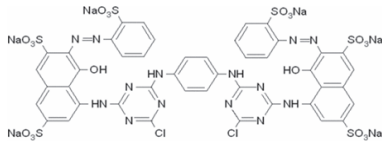
and deposition of these membranes, due to the high hydrophobic properties. Increasing the hydrophilic properties of these membranes can reduce the amount of its obstruction. Several methods that could be used to increase the hydrophilic properties of the membranes surface can be mentioned to grafting some of the hydrophilic chemical groups and defluorination using alkaline chemical solutions [19]. Also, with application of the nano-photocatalyst in the membrane matrix, the self-cleaning properties in the membrane could be created. Nanoparticle powders of semiconductor oxides such as zinc oxide (ZnO) are highly interesting in photocatalytic applications. ZnO has some advantages involving lack of toxicity, high thermal and chemical stability, suitable band-gap energy (E_{bg}) about 3.37 electron volts (eV), high photosensitivity, high catalytic activity, cost-effective and environmentally friendly [20]. ZnO can adsorb photon with sufficient energy (equal to or higher than the band-gap energy) and generating electron (e^-) and hole (h^+) as oxidizing and reducing agents which in this method the mineralization of organic pollutants is not selective [21]. The doping of some metals (Ag, Pd and Pt) and non-metals (N, S and P) in ZnO may cause band-gap energy narrowing, thus nano-photocatalyst activation energy is reduced [22]. Accordingly, contaminants on the membrane surface containing nano-photocatalyst are degraded and the mineralization happened by activation of the nano-photocatalyst in presence of UV irradiation. Subsequently, the obstructions and deposition on the membrane surface are eliminated, due to the presence of oxidant compounds. In the present study, PVDF membrane was prepared in phase inversion by immersion precipitation technique (dry, wet and dry-wet), which is the most common method [23]. In the following membrane, surface modification was performed by chemical method in alkaline conditions in the presence of diethanolamine (DEA) to increase hydrophilic properties of membrane. Then, application of ZnO:Ca as a synthesized photocatalyst in the membrane matrix was investigated in order to use it in a FPMR for dye removal. Finally, self-cleaning properties of nanocomposite membrane was studied under UV irradiation.

2. Experimental setup

2.1. Materials and methods

In the present research, RR120, RB19 and BV16 dyes were used as organic pollutants and high consumption dyes in textile dyeing industries which was purchased from Dycos Co, China (representativeness of Lyafam Chemie Co.) and used without further purification. The chemical structures of all dyes, along with some of their physical properties are given in Table 1. In order to synthesize ZnO:Ca as a nano-photocatalyst, the high purity chemicals were purchased from Merck Co., Germany. These materials include zinc nitrate, glucose, glycine and calcium nitrate hydrate. The applied PVDF for synthesis of polymer membranes was powder and white solid (Kynar 761), which was purchased from Taha Kimia Co. (Iran) with analytical purity grade. N,N-dimethylformamide (DMF), and DEA were also purchased from Merck Co., Germany, with analytical purity grade and used in the experiments. In all required solutions for tests, distilled water was used for preparation of synthetic effluent,

Table 1
Physical and chemical properties of the dyes

Dyes	BV16	RB19	RR120
Molecular weight	368.9428 g mol^{-1}	626.533 g mol^{-1}	1,469.9778 g mol^{-1}
Molecular formula	$C_{23}H_{29}ClN_2$	$C_{22}H_{16}N_2Na_2O_{11}S_3$	$C_{44}H_{30}Cl_2N_{14}O_{20}S_6$
Class	Methine class	Anthraquinones	Double azo class
Nature	Cationic	Anionic	Anionic
Grade	Commercial	Commercial	Commercial
Chemical structure			

but membrane coagulation bath and deionized water were used for the synthesis of photocatalyst nanoparticles. For ZnO:Ca nanoparticles synthesis, combustion method have been used and phase inversion by the immersion precipitation techniques including dry, wet and dry-wet were used for membrane synthesis. Moreover, to increase the hydrophilic properties and membrane surface modification, chemical method was used in alkaline conditions and in the presence of DEA to defluorination of hydrocarbon chain in PVDF.

Decolorization efficiency could be measured using Eq. (1) [24]:

$$\% \text{ Decolorization} = [1 - \left(\frac{C_t}{C_0}\right)] \times 100 \tag{1}$$

where C_0 and C_t are the concentrations at time zero and t, respectively. After membrane synthesis, distilled water was used as a fluid passing through each of the membranes and the permeate flux was calculated using Eq. (2) [25]:

$$J = \frac{Q}{A \cdot T} \tag{2}$$

where J is the permeate (L m^{-2} h^{-1}), Q is the total volume penetrated from the membrane during the membrane separation process (L), T is the effective membrane filtration time (h) and A is the effective area of membrane (m^2).

3. Membrane and nano-photocatalyst synthesis

3.1. Synthesis of ZnO:Ca

In all phases of the synthesis process of ZnO:Ca nano-photocatalyst, high purity chemical materials made by Merck Co., Germany, and deionized water was used. Nano-photocatalyst was synthesized via combustion method in presence of zinc nitrate and glucose as a fuel in deionized water (about 3:1 w/w). Then, calcium nitrate and glycine were added with equal ratio and the sample was heated at 80°C to obtain a yellow gel. Finally, porous white foam was achieved under microwaves (900 W). In order to remove the

remaining gases and generated carbon during combustion, the synthesized sample was heated at 500°C for 1 h at a rate of 10°C/min.

3.2. Synthesis of PVDF membranes

In order to prepare PVDF membrane, phase inversion was used by the immersion precipitation technique (dry, wet and dry-wet) techniques [26,27]. The membrane was made at this stage using hydrophobic polymer materials. There are three ways to prepare membrane by this technique including dry, wet and dry-wet. For making membranes, different % w/w of PVDF (2.5%, 5%, 10%, 20% and 25%) were used as a polymer membrane constructor and DMF as a polymer solvent for polymer matrix production. To eliminate the moisture in the powdery polymer structure, a certain amount of polymer (considering % w/w) was placed in the oven (Memmert, Germany) at 120°C for 3 h before dissolving in the matrix and then cooled at room temperature for 1 h. Afterwards, the polymer and solvent were stirred at room temperature until obtaining a clear solution. The process was performed for 3 h. After the formation of matrix, the solvent was kept constant to remove the formed bubbles resulting from the dissolution. Subsequently, a thin film with 250 μm thickness was placed on a glass plate by film applicator. Then, according to dry production technique, the sample was placed in an oven at 80°C. In the wet production technique, drawn film was placed in the hot water bath at 50°C as a non-solvent. In the combined technique, the sample was dried in oven and then placed in a hot water bath. In this study, we found that 2.5% and 5% (w/w) are not suitable for filming, due to the very low viscosity (matrix high dilution). Also, 25% (w/w) did not produce a uniform film, due to the high viscosity of matrix (high matrix concentration) after filming on the glass plate. According to the observations, application of cold and very hot water (over 80°C) damaged the uniformity of membrane surface and it is not suitable for the center.

3.2.1. Modification of the membrane surface to increase hydrophilicity

As previously mentioned, one of the processes for reduction of the obstruction of the membrane surface is increasing the membrane hydrophilic properties. The surface charge

of the membrane is negative and the membrane made by this polymer is hydrophobic, due to the presence of fluoride groups in the molecular structure of PVDF and its high electronegativity. Removing the fluorine from the structure of polymer would make a significant contribution to its hydrophilic properties. In this process, application of the alkaline conditions inside the polymer matrix before dissolution of PVDF in DMF, a chemical surface modification was performed by the DEA composition at 10, 20, 30 and 40% w/w (DEA to PVDF) and the membrane was prepared as described in section 3.2.

3.2.2. Synthesis of nanocomposite membrane containing ZnO:Ca nanoparticles

Synthesis of the membrane containing of ZnO:Ca nanoparticles was carried out to increase the membrane efficiency. In this regards, to prepare the membrane matrix containing 20% (w/w) polymer, which has been modified with 10% (w/w) DEA, around 0.5, 1, 5, 10, 15 and 20% (w/w) nano-photocatalyst were added to the polymeric matrix. To do this, at first the polymer was placed inside the oven at 120°C during 3 h to remove the moisture in its structure, and then cooled at room temperature for 1 h. Subsequently, 10% (w/w) DEA was added to the polymeric matrix. After complete dissolution of the polymer and the appearance of a clear brown solution, ZnO:Ca nano-photocatalyst with mentioned ratios was added into the polymeric matrix. To have a homogeneous nanoparticle suspension and prevent their aggregation, beaker containing the above compounds was placed inside the ultrasonic apparatus for 30 min (Parsonic Co., Iran). The membrane film was dried during 1 h inside the oven at 80°C, and then placed in a hot water bath at 50°C for 24 h. Before dissolution, the addition of 20% of photocatalyst to the polymer matrix resulted in a very high matrix concentration, which in practice disrupts dissolution of polymer in the solvent and the matrix is not suitable for filming.

4. Results and discussion

4.1. Characterization of ZnO:Ca

4.1.1. X-ray diffraction and FTIR analysis of ZnO:Ca

To confirm the structure of the synthesized nano-photocatalyst and determine the size of its particles, X-ray diffraction (XRD) (PANalytical model X′pert pro-UK) and FTIR spectra (PerkinElmer model Spectrum one, United States) were prepared and are shown in Figs. 1(a) and (b), respectively. XRD pattern was prepared with a scan speed of 0.026° and a wavelength of 0.154 nm at 40 kV and 40 mA to determine the structure. In order to confirm the synthesis of ZnO nanoparticles, the sample was compared with the reference pattern [28]. The size of photocatalyst particles was determined about 30 nm using Scherrer equation (Eq. (3)):

$$D = \frac{0.9\lambda}{\beta Cos\theta} \tag{3}$$

where λ, β and θ are the wavelength of the radiation, total width in half max (0.3°) and half the diffraction angle, respectively [29].

In order to prepare and obtain the FTIR spectrum of ZnO:Ca nanoparticles, the sample was mixed with KBr and by compressing them together, a suitable tablet was prepared for analysis, and the FTIR spectrum was recorded in the range of 450–4,000 cm^{-1}, which is shown in Fig. 1(b). A wide peak was appeared at 3,435.65 cm^{-1} which is related to the O–H bond, the peak appeared in the 1,630.57 cm^{-1} is related to the COO– metal bond. Furthermore, the peak recorded at 543.32 cm^{-1} is related to the metal-oxygen bond.

4.1.2. Photoluminescence spectrum analysis of ZnO:Ca

E_{bg} is one of the most important factors on the efficiency and activation of nano-photocatalyst, which in lower E_{bg} values, the formation of electron–hole pair requires lower energy, which affects the economic efficiency of the nano-photocatalytic process. Accordingly, in order to calculate the E_{bg} of nano-photocatalyst and compare it with the E_{bg} ZnO nano-photocatalyst as a reference, the photoluminescence (PL) of synthesized sample was taken which is shown in Fig. 2 and using Eq. (4) its value was calculated to be 2.31 eV. In comparison with E_{bg} of ZnO nanoparticles (3.37 eV), it can be concluded that the application of calcium as a dopant agents had a significant effect on the reduction of energy of ZnO nano-photocatalytic band [30].
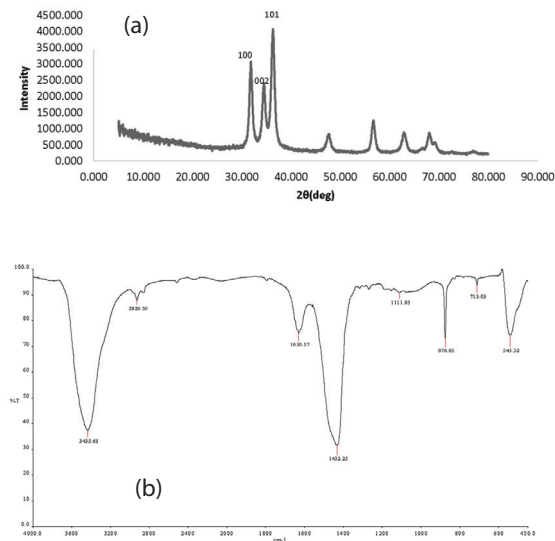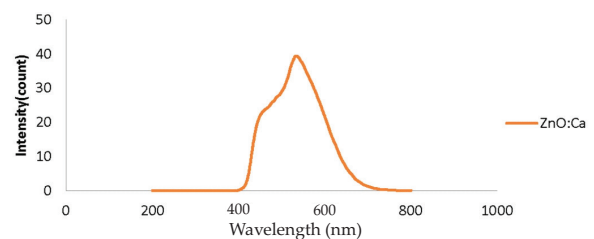

Fig. 1. (a) XRD and (b) FTIR spectra of ZnO:Ca.

Fig. 2. PL spectra of the ZnO:Ca.

$$E_{bg} = \frac{1240}{\lambda} \qquad (4)$$

where E is the energy band gap (eV) and λ is the wavelength (nm).

4.1.3. Mechanism of calcium effect as a dopant agent on reducing E_{bg} of ZnO

In order to confirm the presence of calcium as a dopant agent in the nano-photocatalyst structure of the synthesized ZnO:Ca, the EDX analysis (ZEISS model SIGMA VP-500, Germany) was performed. Furthermore, to investigate the surface morphology of nano-photocatalyst, FESEM (ZEISS model SIGMA VP-500, Germany) images were taken which are shown in Fig. 3. The FESEM images of ZnO:Ca nano-photocatalyst showed the morphology and geometric structure of the synthesized nanoparticles. Accordingly, the geometry of ZnO-Ca nanoparticles is spherical and dense, which the aggregation of nanoparticles together created a porous structure. The EDX analysis of nanoparticles (Fig. 4) confirmed the presence of calcium as a dopant reagent in the structure of the nano-photocatalyst.

In addition, based on the results of the EDX and PL analysis calcium provides active surfaces (Fig. 5). The generated electrons were absorbed which reduced the E_{bg} of nano-photocatalyst.

4.2. Characterization of polymeric membrane

4.2.1. FTIR of pure PVDF and synthetic membranes

FTIR spectra of pure PVDF polymer, PVDF membrane 20% w/w synthesized in dry-wet compound technique, PVDF membrane 20% w/w modified surface with 20% DEA, PVDF membrane 20% w/w surface modified with 20% diethanolamine containing 10% ZnO:Ca nano-photocatalyst were prepared in the range of 450–4,000 cm^{-1} and are shown in Figs. 6(a)–(d).
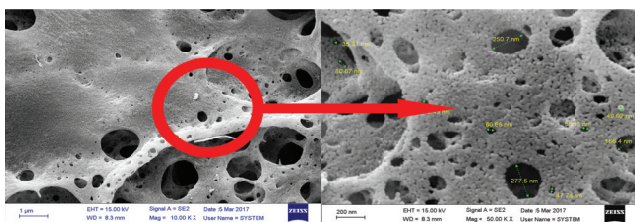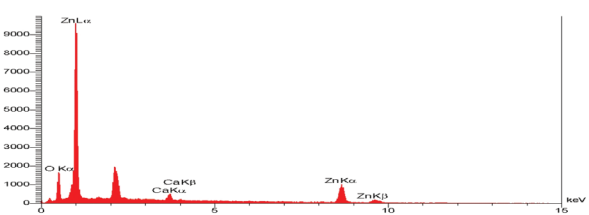

Fig. 3. FESEM of the ZnO:Ca.
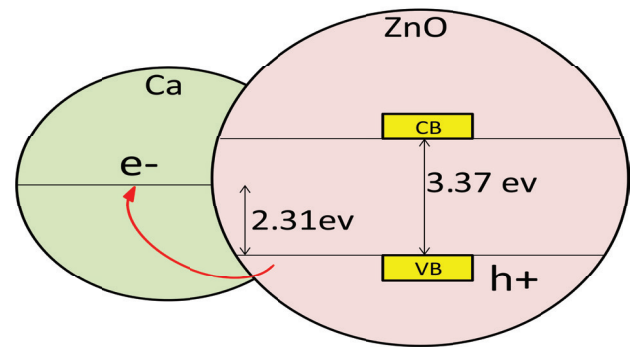

Fig. 4. Analysis EDX ZnO:Ca.

Fig. 5. Effect of calcium in reduce E_{bg} of ZnO in photocatalytic process.
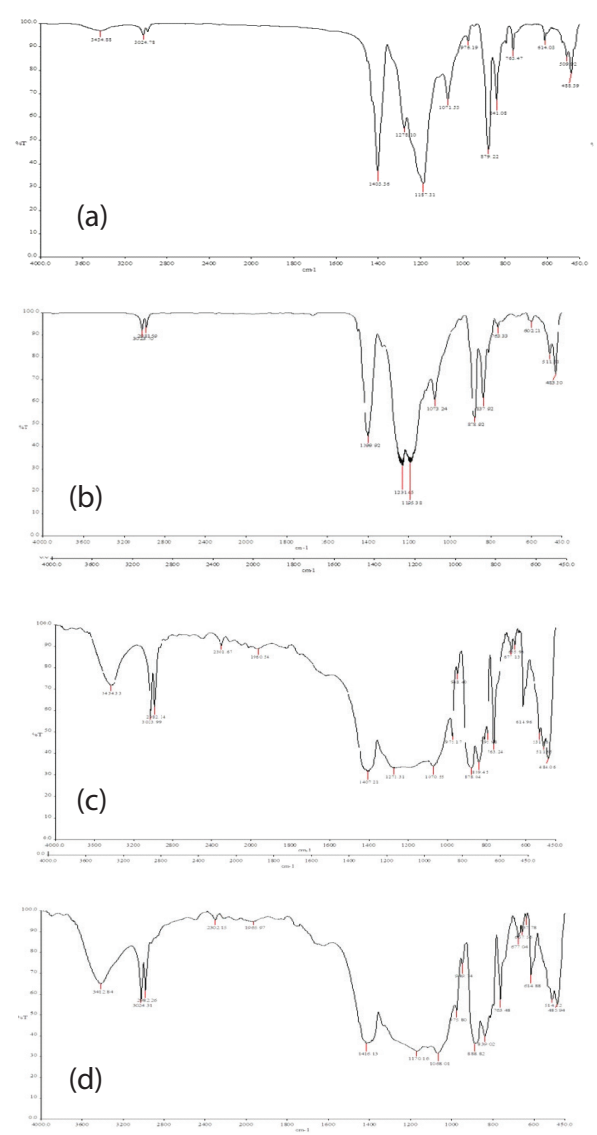

Fig. 6. (a) Pure PVDF, (b) 20% w/w PVDF membrane, (c) 20% w/w PVDF+20% w/w DEA membrane, (d) 20% w/w PVDF+20% w/w DEA+10% w/w ZnO:Ca membrane.

According to Fig. 6(a), peaks appearing at 3,022 cm⁻¹ and 2,980 cm⁻¹ are related to the vibrations of symmetric and asymmetric $-CH_2$ groups in the PVDF molecular structure. The registered peak at 1,187.31 cm⁻¹ is related to the C–C bond in the polymer structure. The present peak at 879.22 cm⁻¹ can be ascribed to C–C–C asymmetric tensile-vibrational bonds and also the recorded peak at 841.08 cm⁻¹ is related to the C–F tensile-vibrational bond in the PVDF polymer structure which corresponds to reference peaks in the sources [31]. According to Fig 6(b), in addition to the presence of pure PVDF peaks, the peak appearing at 1,231.45 cm⁻¹ associated with the asymmetric tensile bond of C–N bond is due to the DMF solvent used as a membrane solvent. In addition, the peak present in the 659–675 cm⁻¹ range (non-peak in comparison with pure PVDF) is related to the O–C–N group in the DMF solvent [32]. Also in Fig. 6(c), in addition to the presence of the peaks, before the recorded peak at 3,434.33 cm⁻¹, is related to the –OH group substitution instead of the fluorine atom in the structure of the PVDF membrane. Also, the broad-band peak that appeared in the range of 1,070.55–1,272.31 cm⁻¹ is related to the C–N tensile bond and the peak at 3,140.20 cm⁻¹, which overlaps with the peak of 3,434.33 cm⁻¹, is related to the N–H bond in the DEA structure. Moreover, the peak appearing in 2,301.67 cm⁻¹ is related to the hydrogen bond with the nitrogen atom. In Fig. 6(d), with minor variations which is due to the presence of ZnO:Ca nanoparticles and its interactions with the atoms and the groups present in the membrane structure, is similar to the spectrum in Fig. 6(c). Changes done in the range of 3,434.33–3,412.48 cm⁻¹ are related to the overlaps of the O–H bond in the ZnO:Ca and –OH nanoparticles of the DEA compound.

4.2.2. FESEM (cross-section) and EDX analysis of synthetic membranes

After synthesis of 20% PVDF membranes, 20% PVDF modified with 20% DEA and 20% surface modified PVDF membrane with 20%DEA containing 10% ZnO:Ca synthetic nano-photocatalyst in phase inversion method (dry-wet), synthetic samples were frozen in the liquid nitrogen, then a small piece of it was broken and prepared for their cross-sectional imaging. The FESEM images of the synthetic samples are shown in Figs. 7(a)–(c). In order to suggest a mechanism for increasing the membrane hydrophilicity and confirming the presence of ZnO:Ca nano-photocatalyst, the synthetic samples were analyzed by EDX analysis and the results are shown in Figs. 8(a)–(c).

The FESEM images (Fig. 7(c)) show the presence of nanoparticles in the membrane structure. Also, based on these images, it can be postulated that all three synthesized membranes are placed in a dense membrane group.

Based on the EDX analysis of membranes (Figs. 8(a)–(c)), it was determined that the peak intensity of the fluorine element in the surface-modified membranes and the surface-modified composite content of the ZnO:Ca nanoparticles was decreased which indicated that the chemical surface modification by diethanolamine had a dramatic effect on defluorination. By comparing Figs. 8(b) and (c), it can be seen that despite the same content of DEA in both polymeric matrix, defluorination in the polymeric matrix in the presence of ZnO:Ca is less than the others. According to Reactions
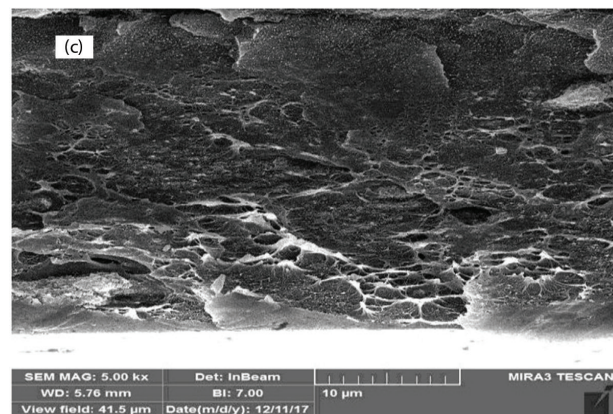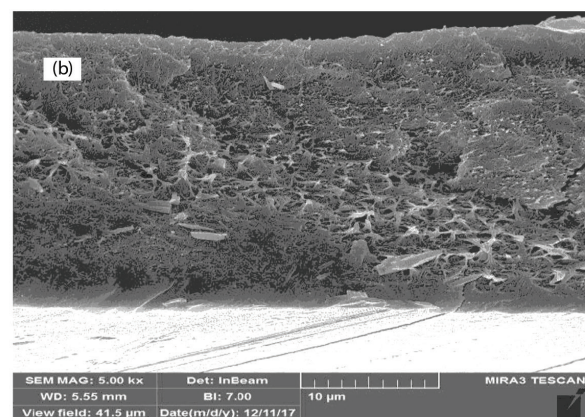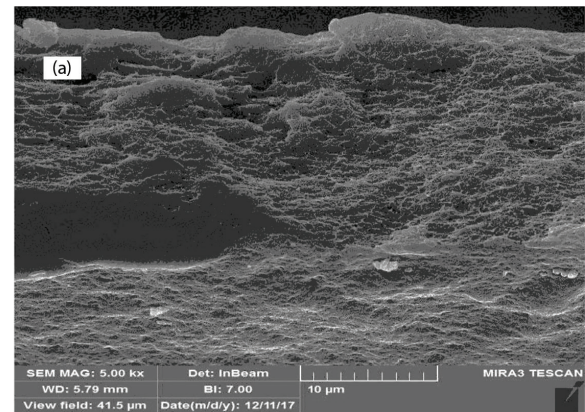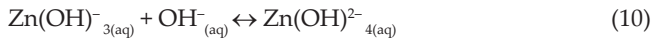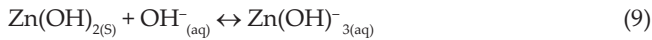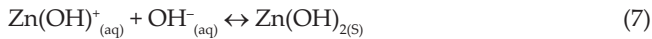

Fig. 7. FESEM (a) 20% w/w PVDF membrane, (b) 20% w/w PVDF+20% w/w DEA membrane, (c) 20% w/w PVDF+20% w/w DEA+10% w/w ZnO:Ca membrane.

(5)–(10), ZnO is reacted in alkaline solution with hydroxide ion (OH⁻). Therefore, a part of the OH⁻ in the polymer matrix reacts with ZnO, instead of attacking the hydrocarbon chain of PVDF and defluorination [33]. Thus, a lower amount of the fluorine was separated from the hydrocarbon chain and subsequently its peak intensity was increased in EDX.

$$ZnO_{(s)} \leftrightarrow Zn^{2+}_{(aq)} + O^{2-}_{(aq)} \tag{5}$$

$$Zn^{2+}_{(aq)} + OH^-_{(aq)} \leftrightarrow Zn(OH)^+_{(aq)} \tag{6}$$

$$Zn(OH)^+_{(aq)} + OH^-_{(aq)} \leftrightarrow Zn(OH)_{2(S)} \qquad (7)$$

$$Zn(OH)_{2(S)} \leftrightarrow Zn(OH)_{2(aq)} \qquad (8)$$

$$Zn(OH)_{2(S)} + OH^-_{(aq)} \leftrightarrow Zn(OH)^-_{3(aq)} \qquad (9)$$

$$Zn(OH)^-_{3(aq)} + OH^-_{(aq)} \leftrightarrow Zn(OH)^{2-}_{4(aq)} \qquad (10)$$

4.3. Atomic force microscopy analysis of synthetic PVDF membranes

To determine the roughness and smoothness of synthetic membrane surfaces, their surfaces were investigated by atomic force microscopy (AFM) technique (it should be noted that due to the prominence caused by the presence of ZnO:Ca photocatalytic nanoparticles on the membrane surface, the preparation of AFM images of this sample is

Fig. 8. EDX (a) 20% w/w PVDF membrane, (b) 20% w/w PVDF+20% w/w DEA membrane, (c) 20% w/w PVDF+20% w/w DEA+10% w/w ZnO:Ca membrane.

not possible). Based on the images shown in Figs. 9 and 10, the degree of roughness of the surface-modified membrane has significantly decreased from 768 nm (PVDF) to 428 nm (PVDF-DEA) that is due to the removal of fluorine atoms from hydrocarbon chain. Reducing the roughness of the membrane surfaces means less adhesion to the pollutants, which resulted in reduction of obstruction and surface deposition of the membrane.

4.4. Estimating the amount of permeate

After membrane synthesis, to investigate the mechanical strength of the synthetic membranes against the fluid pressure, samples with different of 10, 15 and 20% w/w were prepared by means of three dry, wet and dry-wet techniques and placed inside the membrane system under 2–4 times pressure. In this part of the experiments, distilled water was used as a fluid in the dead-end membrane system, and the results of this test are presented in Table 2.

Based on the results of the test, it is determined that membranes containing 20% w/w PVDF have a much higher resistance to 10 and 15% vs. flow fluid. Accordingly, 20% w/w PVDF concentration was considered as a suitable concentration for membrane synthesis in the next steps.

4.5. Determination of the hydrophilicity property of synthetic membranes

One of the characteristics of the membranes to reduce the membrane obstruction is reduction of its hydrophobic properties. The contact angle analysis determines the degree of hydrophilicity and hydrophobicity of the synthetic membranes in various ways. For this purpose, the contact
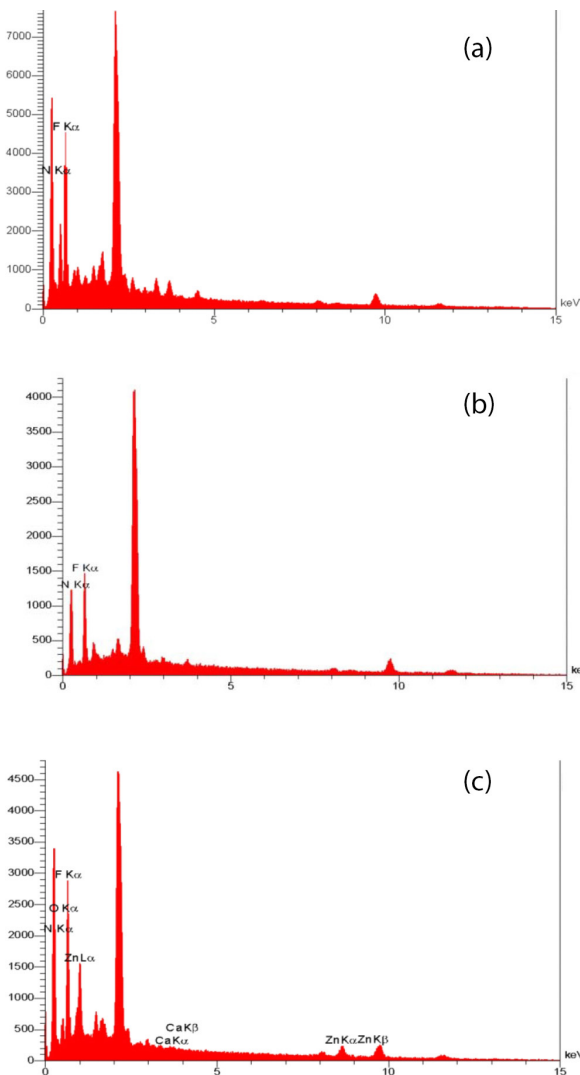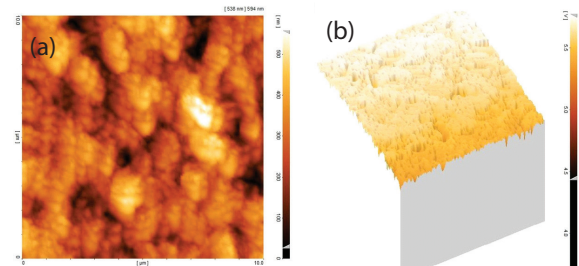

Fig. 9. AFM 20% w/w PVDF membrane: (a) two-dimensional and (b) three-dimensional.
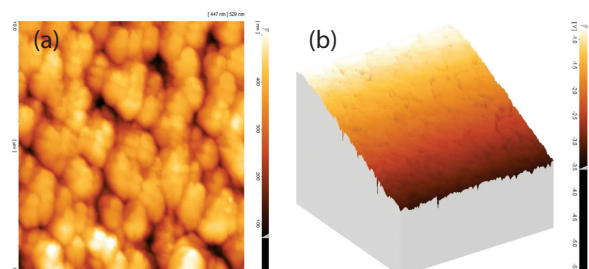

Fig. 10. 20% w/w PVDF+20% w/w DEA membrane (a) two-dimensional and (b) three-dimensional.

Table 2
Evaluation of the stability of synthetic membranes against applied pressure

| Results	Membrane diameter (cm)	Pressure (bar)	Membrane making technique	(% w/w)
Non-resistance to pressure	9	2–4	Dry (oven 80°C)	10
Non-resistance to pressure	9	2–4	Dry (oven 80°C)	15
Resistance to pressure	9	2–4	Dry (oven 80°C)	20
Non-resistance to pressure	9	2–4	Wet (water bath 50°C)	10
Non-resistance to pressure	9	2–4	Wet (water bath 50°C)	15
Resistance to pressure	9	2–4	Wet (water bath 50°C)	20
Non-resistance to pressure	9	2–4	Dry-wet (oven–hot water bath)	10
Non-resistance to pressure	9	2–4	Dry-wet (oven–hot water bath)	15
Resistance to pressure	9	2–4	Dry-wet (oven–hot water bath)	20
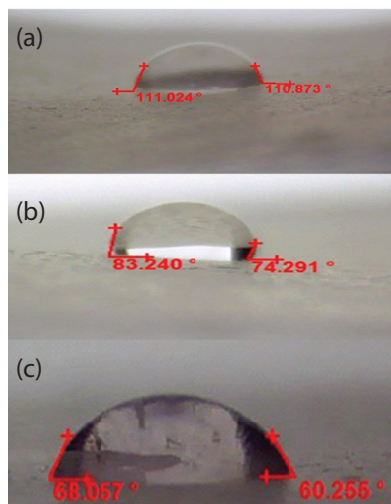
Fig. 11. Contact angle analysis (a) 20% w/w PVDF membrane (dry), (b) 20% w/w PVDF membrane (wet) and (c) 20% w/w PVDF membrane (dry-wet).

angle analysis was performed on three membranes resistant to the operating pressure in the process (2–4 bar), which performed by testing for the stability and resistance of the membranes synthesized in the membrane system. Results are presented in Figs. 11(a)–(c), which are related to the synthetic membrane of 20% PVD by dry, wet and dry-wet techniques.

Results of the contact angle tests showed that the moisture content of the 20% w/w PVDF membrane hydrophilicity synthesized by dry-wet technique was higher than wet and dry techniques, because the contact angle has increased (average) from 64.16° to 78.76° and 110.94°, respectively. Using this technique (dry-wet), the solvent was evaporated at the short time and water as a non-solvent permeated in membrane. So combination of these techniques increased hydrophilicity property of membrane.

Therefore, it can be concluded that this technique (dry-wet) is the most suitable one for synthesis of the membrane in order to increase its hydrophilic property. This analysis also showed that the application of water during the final synthesis of the membrane as a non-solvent caused increase in the permeability of the membrane to water.

4.5.1. Study of permeate of synthetic membranes

In this experiment, to determine the amount of permeate and the water absorption of synthetic membranes in dry, wet and dry-wet techniques, distilled water was studied as a fluid and its passage from each of the synthesized membranes was investigated as a permeate. In this regard, synthetic membranes with a diameter of 9 cm were prepared and used at operating pressure of 2–4 bar within the dead-end membrane system. Results of this study are presented in Table 3 and Fig. 12. Based on the results of stability test in the dead-end membrane system, a synthesized membrane by dry-wet technique is a suitable technique for membrane synthesis in the next steps of the relevant experiments, due to reducing contact angle and increasing permeate.

4.6. Modification of the membrane surface to increase hydrophilicity

One of the processes that reduces the obstruction of the surface of the membrane is increasing the membrane hydrophilicity. Removal of fluorine from the structure of this polymer can make a significant contribution to its hydrophilic properties. In this experiment, the defluorination has been considered using chemical method with an alkaline solution. By providing the alkaline conditions inside the polymer matrix before dissolving polyvinylidene fluoride in DMF by DEA composition in of 10, 20, 30 and 40% w/w (DEA to polymer), permeate from the modified membranes was investigated. In this experiment, distilled water was used as a fluid flow. Results of this experiment are presented in Table 4 and Fig. 13. The results of this test showed that the synthesized membrane with 20% w/w of DEA has a higher permeate, compared with other synthetic membranes which is the same as the optimum ratio used in the synthesis of the membranes in the next sections. Using excessive DEA, the amount of OH^- ions in polymeric matrix is decreased, because the desire OH^- ions are increased and recombined into the DEA structure. Accordingly, the amount of OH^- ions attacking the structure of hydrocarbons is reduced. Subsequently, less fluorine atoms will be removed from the chain.

In the following, to determine the hydrophilicity of the modified synthetic membrane with a 20% DEA was analyzed by contact angle analysis. The analysis of the contact angle of the membrane is shown in Fig. 14. Results revealed that

Table 3
Effect of synthesis technique on permeate flux

Permeate (mL cm^{-2} s^{-1})	Time (s)	Volume of water (mL)	Absorbed water mass (g)	Wet membrane mass (g)	Dry membrane mass (g)	Pressure (bar)	Membrane surface area (cm^2)	Membrane synthesis technique
0.0084	465	250	0.0557	0.3755	0.3198	2–4	63.585	Dry
0.009	433	250	0.0856	0.3887	0.3031	2–4	63.585	Wet
0.01	382	250	0.1486	0.4654	0.3168	2–4	63.585	Dry-wet

Table 4
Optimum ratio of DEA

| Permeate (mL cm^{-2} s^{-1})	Time (s)	Volume of water (mL)	Absorbed water mass (g)	wet membrane mass (g)	Dry membrane mass (g)	Pressure (bar)	Membrane surface area (cm^2)	%DEA	Membrane synthesis technique
0.018	211	250	0.0697	0.4308	0.3611	2–4	63.585	10	Dry-wet
0.025	153	250	0.1075	0.4831	0.3756	2–4	63.585	20	Dry-wet
0.016	248	250	0.0619	0.4501	0.3882	2–4	63.585	30	Dry-wet
0.015	255	250	0.0554	0.4498	0.3944	2–4	63.585	40	Dry-wet
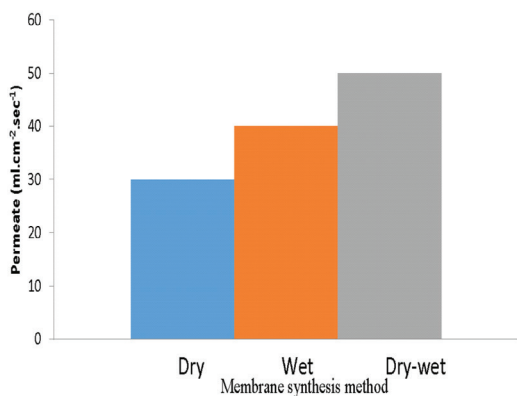
Fig. 12. Investigation of permeate relative to the construction technique.

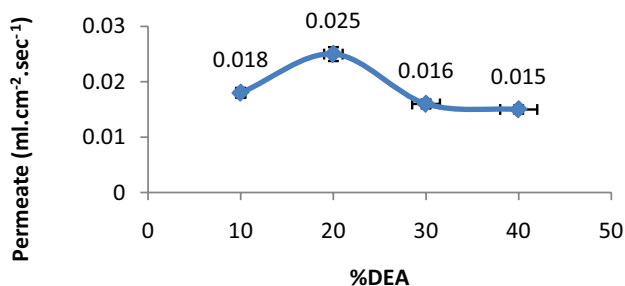Fig. 13. Optimum amount of DEA.

Fig. 14. Contact angle of modified membrane by 20% w/w DEA.

the contact angle was reduced to about (average) 58.83°, indicating an increase in the membrane hydrophilicity (removed fluorine groups).

Subsequently, the permeate from the membrane containing ZnO:Ca as a photocatalytic nanoparticles was investigated in a similar way as before and the results are presented in Table 5 and Fig. 15.
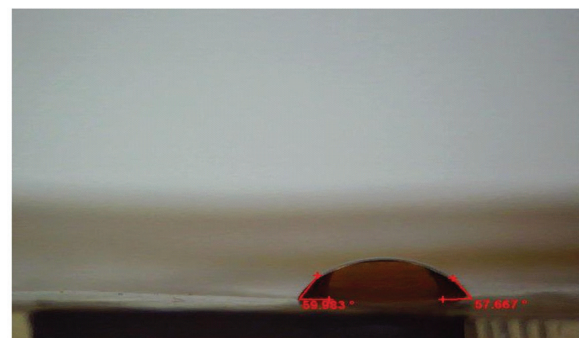
In the next steps, for determination of the hydrophilicity of the modified synthetic membrane with 20% of DEA and 10% w/w of nano-photocatalyst, contact angle analysis was performed.

The results of contact angle analysis of the membrane (Fig. 16) show that increasing the % w/w of photocatalyst nanoparticles up to 10 % (w/w) not only caused reduction of the contact angle to 46.414°, which means increasing the hydrophilicity of the membrane and the amount of charge flowing, but also increased the % w/w of ZnO:Ca nanoparticles which led to decreasing the amount of flowing fluids due to the obstruction of canals and membrane cavities by nanoparticles. Accordingly, the optimal amount of nano-photocatalyst is 10% (w/w).

4.7. Mechanism of surface modification by chemical method

According to the results of EDX analysis, the reduction of peak intensity of fluorine in both surface-modified membranes and the PVDF/ZnO:Ca, as a nano-composite, and the presence of –OH group in the molecular structure of the membrane which confirms the FTIR spectrum shown in Fig. 6(c), as well as the reduction of contact angle, it can

Table 5
Effect of ZnO:Ca ratio on permeate flux

Permeate (mL cm^{-2} s^{-1})	Time (s)	Volume of water (ml)	Absorbed water mass (g)	wet membrane mass (g)	Dry membrane mass (g)	Pressure (bar)	Membrane surface area (cm^2)	%ZnO:Ca	Membrane synthesis technique
0.018812	209	250	0.0791	0.4412	0.3621	2–4	63.585	0.5	Dry-Wet
0.020914	188	250	0.1189	0.4852	0.3663	2–4	63.585	1	Dry-Wet
0.02693	146	250	0.125	0.4981	0.3731	2–4	63.585	5	Dry-Wet
0.029786	132	250	0.1312	0.5210	0.3898	2–4	63.585	10	Dry-Wet
0.02006	196	250	0.1421	0.5731	0.431	2–4	63.585	15	Dry-Wet
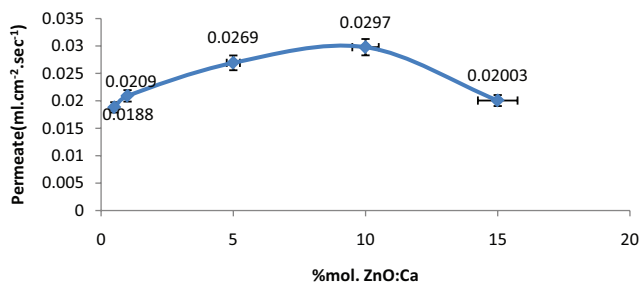
Fig. 15. Optimum amount of ZnO:Ca.

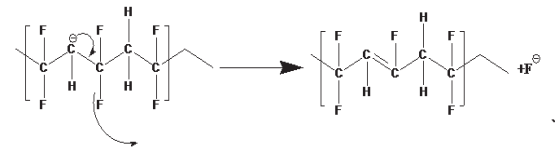Fig. 16. Contact angle of modified membrane by 20% w/w DEA+10% ZnO:Ca.

Fig. 17. Chemical modification mechanism.

4.8. Evaluation of the performance of PVDF membranes on the removal efficiency of RR120, RB19 and BV16 dyes

To investigate the removal efficiency of RR120, RB19 and BV16 dyes by 20% synthesized PVDF membranes using dry-wet technique, 20% PVDF surface-modified with 20% DEA synthesized using dry-wet technique and 20% synthesized PVDF to increase the hydrophilicity with 20% w/w of DEA and content of 10% ZnO:Ca by dry-wet technique and to evaluate their efficiency, solutions with concentration of 10 mg L^{-1} were prepared and in a dead-end membrane system with a diameter of 9 cm, the schematic shape of the related set up has been shown in Fig. 18. The results of this test are shown in Figs. 19(a)–(c).

Based on Figs. 19(a)–(c), it is obvious that the removal of RR120 and RB19 dyes is much lower than that of BV16 dye. The removal efficiencies of these dyes were calculated to be 3.84%, 2.61% and 37.52%, respectively. Considering the negative surface of 20% w/w of synthetic PVDF membrane and its high hydrophobic properties, due to the presence of fluorine groups, as well as the anionic features of the RR120 and RB19 dyes, it can be explained that with interaction between the surface of the membrane and the two dyes, due to the same electrostatic charges, the PVDF membrane of the unmodified surface does not succeed in isolating them from synthetic effluent, which caused the very low efficiency of dye removal. However, regarding the cationic characteristics of BV16 dye, there is a physical bond between the dense molecular structure and the membrane surface, which improves the efficiency of the synthetic membrane in dye removal. Its high removal efficiency (37.52%), compared with

be concluded that the OH$^-$ released group in the solution resulting from the application of DEA in the polymer matrix, as described in Fig. 17, has the eliminating effect on the fluorine groups in the polymeric chain. Accordingly, the removal of fluorine from the membrane structure has increased its hydrophilic properties. The proposed mechanism is a two-step reaction. In the first step, OH$^-$ ion caused the formation of –CH$^-$ in the polymer structure thereby separating a hydrogen atom from the hydrocarbon chain and producing water. Due to the equilibrium of DEA ionization, increasing the use of DEA increases the concentration of OH$^-$ which results in the reaction being returned, that the result is a reduction in the OH$^-$ in the reaction, which ultimately leads to a reduction in the removal of polymer fluoride atoms. In the second step, the formation of double bond between two carbons in the hydrocarbon chain causes removed fluorine.

the two dyes RR120 and RB19 confirms the efficiency of membrane function. By improvement of the membrane surface, the removal efficiencies of the RR120, RB19 and BV16 dyes were increased to 10.75%, 14.05% and 57.42%, respectively, which confirmed increasing the membrane hydrophobic properties and removal of fluorine groups from hydrocarbon

chain. By addition of ZnO:Ca nanoparticles, the removal efficiencies of RR120, RB19 and BV16 dyes were increased to 18.45%, 27.36% and 66.45 %, which proved that the addition of ZnO:Ca nanoparticles to the membrane matrix has been successful in order to improve the membrane hydrophilic properties.
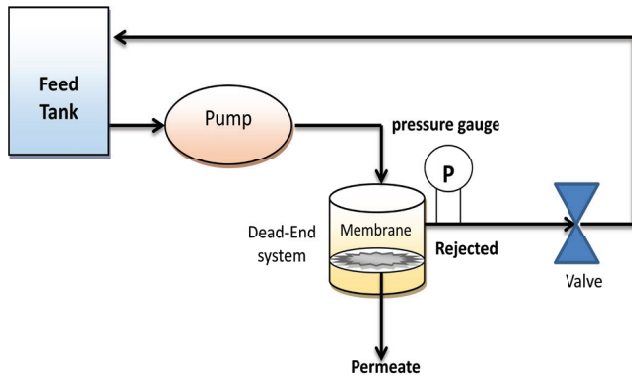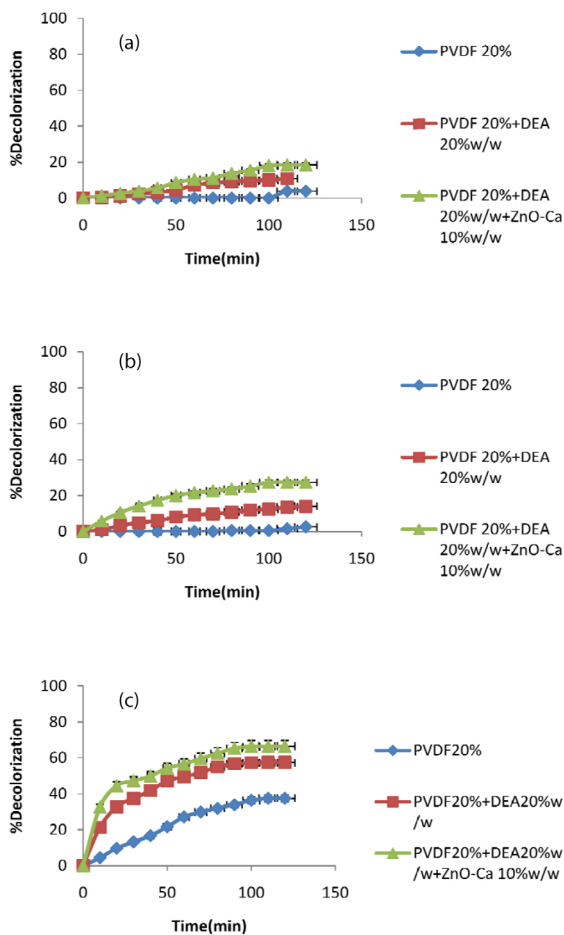
4.9. Study of the performance of FPMR on the dye removal efficiency of RR120, RB19, BV16 and self-cleaning properties of the PVDF/ZnO:Ca

The effect of UV irradiation, photocatalyst and polymeric membrane on the decolorization efficiency of RR120, RB19 and BV16 dyes was simultaneously investigated within a FPMR which its schematic design is shown in Fig. 20. 10 mg L^{-1} dye solutions with neutral pH and 5.5 L min^{-1} aeration rate were prepared at room temperature.

Initially, duration passing distilled water from the membrane was measured from 20% PVDF surface-modified membrane with 20% DEA containing 10% ZnO:Ca as a nano-photocatalyst, synthesized in dry-wet technique and each of the dye solutions was then passed 10 times through it and the time was recorded after each passing. The results of this test are shown in Figs. 21 and 22.

Based on the obtained results, it is observed that the removal efficiencies of RR120, RB19 and BV16 dyes in the FPMR are 65.10%, 75.95% and 65.04%, respectively, during 1 h and the high percentage of dyes has been removed from the individual dead-end membrane system. Furthermore, in order to study the self-cleaning properties of the PVDF/ZnO:Ca as a nano-composite membrane, the duration of passing distilled water through the membranes

Fig. 18. Dead-end membrane set-up.

Fig. 19. (a) Evaluation of the efficacy of synthetic membrane on removal of RR120, (b) RB19 and (c) BV16.
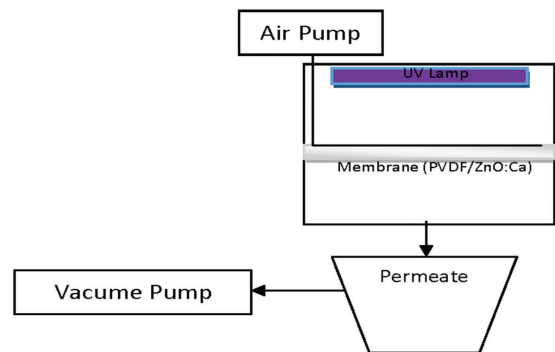

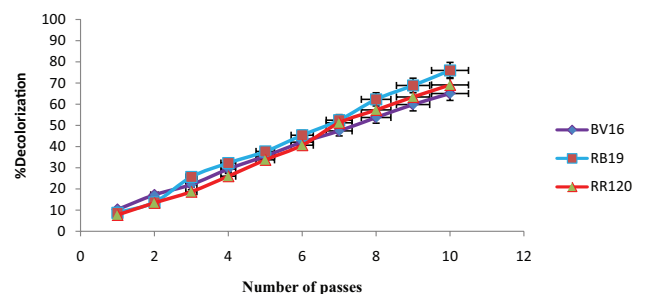Fig. 20. Fixed-bed photocatalytic-membrane reactor.

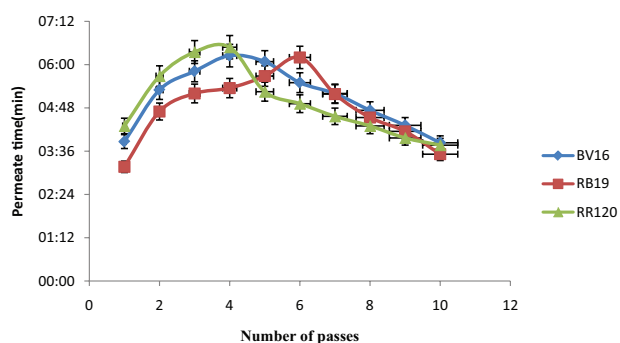Fig. 21. Removal efficiency of RR120, RB19 and BV16 in the FPMR.

Fig. 22. Evaluation of the self-cleaning property of synthetic modified membrane content nano-photocatalyst.

which used to remove any of the RR120, RB19 and BV16 dyes in the FPMR before the beginning of the process was determined 3:41, 3:12 and 3:20. The obtained results in Fig. 22 show that for all three dyes, the passage time was increased in parallel with the passing frequency, but with increase in exposure to PVDF/ZnO:Ca (increasing the frequency of passing), the passing time of each dyes has decreased which suggests that the molecular structure of the dye located on the membrane surface has been reduced, indicating that the molecular structure of the dye located on the membrane surface was destroyed by photocatalyst nanoparticles activated by UV irradiation and the obstruction of membrane was decreased. These reactions resulted in the reduction of the passing time of the dye solution through the nano-composite membrane.

5. Conclusion

Based on the results of analysis of synthetic membranes, it can be concluded that membrane synthesis by phase inversion method (dry-wet) is an effective way to improve the hydrophilic properties of membranes that are made by hydrophobic polymers. The modification of the synthetic membrane of 20% PVDF by using DEA provided an alkaline environment which effectively eliminated the fluorine groups from the polymer chain and increased its hydrophilic properties. Synthesis of ZnO:Ca nanoparticles was performed by combustion method for synthesis of nano-composite membrane and its application into fixed-bed photocatalytic-membrane reactor. By addition of nano-photocatalyst to the membrane matrix and synthesis of the nano-composite membrane, the hydrophilic properties of hydrophobic PVDF membrane increased significantly. The nano-composite membrane (nonuse of UV light) was more effective for removal of BV16 dye than the two other dyes. The removal efficiency of RR120, RB19 and BV16 dyes within the FPMR was much more efficient than the dead-end membrane system and yielded high efficiencies in removing all three dyes at a shorter time period (1 h).

References

[1] P. Velmurugan, V. Rathina kumar, G. Dhinakaran, Dye removal from aqueous solution using low cost adsorbent, Int. J. Environ. Sci., 1 (2011) 1492–1503.

[2] J.M. Salman, M.A. Baiee, A.R. Omran, Experimental study to removal of methylene blue dye from aqueous solution by adsorption on eco-friendly materials, Int. J. ChemTech. Res., 9 (2016) 560–566.

[3] V.M. Sivakumar, M. Thirumarimurugan, A.M. Xavier, A. Sivalingam, T. Kannadasan, Colour removal of direct red dye effluent by adsorption process using rice husk, Int. J. Biosci. Biochem. Bioinf., 2 (2012) 377–380.

[4] M.T. Amin, A.A. Alazba, M. Shafiq, Adsorptive removal of reactive black 5 from wastewater using bentonite clay: isotherms, kinetics and thermodynamics, Sustainability, 7 (2015) 15302–15318.

[5] T.W. Gebreslassie, M. Pattabi, R.M. Pattabi, Review on the photocatalytic degradation of dyes and antibacterial activities of pure and doped-ZnO, Int. J. Sci. Res., 4 (2015) 2252–2264.

[6] V.C. Padmanaban, S. Jose, C. Rapheal, Reactor systems for the degradation of textile dyes, Int. J. Environ. Sci., 3 (2013) 1868–1873.

[7] M.E. Olya, H.A. Pirkarami, M. Soleimnai, N. Yousefi Limaee, Decomposition of a diazo dye in aqueous solutions by $KMnO_4$ / UV/H_2O_2 process, Prog. Color Colorants Coat., 5 (2012) 41–46.

[8] C.C. Liu, Y.H. Hasieh, P.F. Li, C.H. Li, C.L. Kao, Photodegradation treatment of azo dye wastewater by UV/TiO_2 process, Dyes Pigm., 68 (2006) 191–195.

[9] S. Mozia, Photocatalytic-membrane reactors (PMRs) in water and wastewater treatment. A review, Sep. Purif. Technol., 73 (2010) 71–91.

[10] D. Darowna, R. Wroble, A.W. Morawski, S. Mozia, The influence of feed composition on fouling and stability of a polyethersulfone ultrafiltration membrane in a photocatalytic-membrane reactor, Chem. Eng. J., 310 (2017) 360–367.

[11] M. Rajca, The effectiveness of removal of nom from natural water using photocatalytic-membrane reactors in PMR-UF and PMR-MF modes, Chem. Eng. J., 305 (2016) 169–175.

[12] R. Molinari, C. Lavorato, P. Argurio, Recent progress of photocatalytic-membrane reactors in water treatment and in synthesis of organic compounds, a review, Catal. Today, 281 (2017) 144–164.

[13] J. Grzechulska-Damszel, M. Tomaszewska, A.W. Morawski, Integration of photocatalysis with membrane processes for purification of water contaminated with organic dyes, Desalination, 241 (2009) 118–126.

[14] S. Chin, K. Chiang, A. Fane, The stability of polymeric membranes in a TiO_2 photocatalysis process, J. Membr. Sci., 275 (2006) 202–211.

[15] M. Matsuda, K. Yamamoto, T. Yakushijii, M. Fukuda, T. Miyasaka, K. Sakai, Nanotechnological evaluation of protein adsorption on dialysis membrane surface hydrophilized with polyvinylpyrrolidone, J. Membr. Sci., 310 (2008) 219–228.

[16] D.J. Lin, C.L. Chang, T.C. Chen, L.P. Cheng, On the Structure of Porous Poly(vinylidene fluoride) Membrane Prepared by Phase Inversion from Water-NMP-PVDF System, Tamkang J. Sci. Eng., 5 (2002) 95–98.

[17] Q. Zhang, X. Lu, L. Zhao, Preparation of PVDF(PVDF) hollow fiber hemodialysis membranes, Membranes (Basel), 4 (2014) 81–95.

[18] H. Bai, X. Wang, Y. Zhou, L. Zhang, Preparation and characterization of poly(vinylidenefluoride) composite membranes blended with nano-crystalline cellulose, Prog. Nat. Sci. Mater. Int., 22 (2012) 250–257.

[19] A. Du Pasquier, P.C. Warren, D. Culver, A.S. Gozdz, J.J. Amatucci, J.M. Tarascon, Plastic PVDF-HFP electrolyte laminates prepared by a phase-inversion process, Solid State Ion., 135 (2000) 249–257.

[20] R. Slama, J. El Ghoul, K. Omri, A. Houas, L. El Mir, F. Launay, Effect of Ca-doping on microstructure and photocatalytic activity of ZnO nanoparticles synthesized by sol gel method, J. Mater. Sci., 27 (2016) 7939–7946.

[21] U.G. Akpan, B.H. Hameed, Parameters affecting the photocatalytic degradation of dyes using TiO_2-based photocatalysts: a review, J. Hazard. Mater., 170 (2009) 520–529.

[22] R.C. Pawar, D.H. Choi, J.S. Lee, C.S. Lee, Formation of polar surfaces in microstructured ZnO by doping with Cu and

applications in photocatalysis using visible light, Mater. Chem. Phys., 151 (2015) 167–180.

[23] X. Hea, C. Chenb, Z. Jiangc, Y. Suc, Computer simulation of formation of polymeric ultrafiltration membrane via immersion precipitation, J. Membr. Sci., 371 (2011) 108–116.

[24] A. Pokharia, S.S. Ahluwalia, Decolorization of xenobiotic azo dye- black WNN by immobilized *Paenibacillus alvei* MTCC 10625, Int. J. Environ. Biorem. Biodegrad., 4 (2016) 35–46.

[25] L. Yang, B. Tang, P. Wu, UF membrane with highly improved flux by hydrophilic network between graphene oxide and brominated poly (2,6-dimethyl-1,4-phenylene oxide), J. Mater. Chem. A Mater., 2 (2014) 18562–18573.

[26] F. Liu, N. Awanis Hashim, Y. Liu, M.R. Moghareh Abed, K. Li, Progress in the production and modification of PVDF membranes, J. Membr. Sci., 375 (2011) 1–27.

[27] J.H. Kim, B.R. Min, J. Won, H.C. Park, Y.S. Kang, Phase behavior and mechanism of membrane formation for polyimide/DMSO/water system, J. Membr. Sci., 187 (2001) 47–55.

[28] N. Assi, P. Aberoomand Azar, M.S. Tehrani, S.W. Husain, M. Darwish, S. Pourmand, Synthesis of ZnO-nanoparticles by microwave assisted sol-gel method and its role in photocatalytic degradation of food dye Tartrazine (Acid Yellow 2), Int. J. Nano Dimens., 8 (2017) 241–249.

[29] M.A. Khan, M. Siddique, F. Wahid, R. Khan, Removal of reactive blue 19 dye by sono, photo and sonophotocatalytic oxidation using visible light, Ultrason. Sonochem., 26 (2015) 370–377.

[30] R.J. Tayade, P.K. Surolia, R.J. Kulkarni, P.V. Jasra, Photocatalytic degradation of dyes and organic contaminants in water using nanocrystalline anatase and rutile TiO_2, Sci. Technol. Adv. Mater., 8 (2007) 455–462.

[31] S. Gu, G. He, X. Wu, Z. Hu, L. Wang, G. Xiao, L. Pemg, Preparation and characterization of poly (vinylidene fluoride)/sulfonated poly (phthalazinone ether sulfone ketone) blends for proton exchange membrane, J. Appl. Polym. Sci., 116 (2010) 852–860.

[32] W. Ma, J. Zhang, S. Chen, X. Wang, Crystalline phase formation of poly(vinylidene fluoride) from tetrahydrofuran/N,N-dimethylformamide mixed solutions, J. Macromol. Sci. B, 47 (2008) 434–449.

[33] F.M. Omar, H.A. Aziz, S. Stoll, Stability of ZnO nanoparticles in solution. Influence of pH, dissolution, aggregation and disaggregation effects, J. Colloid Sci. Biotechnol., 3 (2014) 1–10.